

## A new mixed mode I/II failure criterion for laminated composites considering fracture process zone

Daneshjoo, Z.; Shokrieh, M. M.; Fakoor, M.; Alderliesten, R. C.

**DOI**

[10.1016/j.tafmec.2018.09.004](https://doi.org/10.1016/j.tafmec.2018.09.004)

**Publication date**

2018

**Document Version**

Accepted author manuscript

**Published in**

Theoretical and Applied Fracture Mechanics

**Citation (APA)**

Daneshjoo, Z., Shokrieh, M. M., Fakoor, M., & Alderliesten, R. C. (2018). A new mixed mode I/II failure criterion for laminated composites considering fracture process zone. *Theoretical and Applied Fracture Mechanics*, 98, 48-58. <https://doi.org/10.1016/j.tafmec.2018.09.004>

**Important note**

To cite this publication, please use the final published version (if applicable). Please check the document version above.

**Copyright**

Other than for strictly personal use, it is not permitted to download, forward or distribute the text or part of it, without the consent of the author(s) and/or copyright holder(s), unless the work is under an open content license such as Creative Commons.

**Takedown policy**

Please contact us and provide details if you believe this document breaches copyrights. We will remove access to the work immediately and investigate your claim.

© 2018 Manuscript version made available under CC-BY-NC-ND 4.0 license  
<https://creativecommons.org/licenses/by-nc-nd/4.0/>

## A new mixed mode I/II failure criterion for laminated composites considering fracture process zone

Z. Daneshjoo<sup>a</sup>, M.M. Shokrieh<sup>a,\*</sup>, M. Fakoore<sup>b</sup>, R.C. Alderliesten<sup>c</sup>

<sup>a</sup>Composites Research Laboratory, Center of Excellence in Experimental Solid Mechanics and Dynamics, School of Mechanical Engineering, Iran University of Science and Technology, Tehran, 16846-13114, Iran

<sup>b</sup>Faculty of New Sciences and Technologies, University of Tehran, Tehran, 14395-1561, Iran

<sup>c</sup>Structural Integrity & Composites Group, Faculty of Aerospace Engineering, Delft University of Technology, Kluyverweg 1, 2629HS Delft, The Netherlands

\*(Corresponding author: [Shokrieh@iust.ac.ir](mailto:Shokrieh@iust.ac.ir))

### Abstract

In this paper, by considering the absorbed energy in the fracture process zone and extension of the minimum strain energy density theory for orthotropic materials, a new mixed mode I/II failure criterion was proposed. The applicability of the new criterion, to predict the crack growth in both laminated composites and wood species, was investigated. By defining a suitable damage factor and using the mixed mode I/II micromechanical bridging model, the absorbed energy in the fracture process zone was considered. It caused the new criterion to be more compatible with the nature of the failure phenomena in orthotropic materials unlike available ones that were conservative. A good agreement was obtained between the fracture limit curves extracted by the present criterion and the available experimental data. The theoretical results were also compared with those of the minimum strain energy density criterion to show superiority of the newly

proposed criterion.

**Keywords:** Failure criterion, Strain energy density theory, Laminated composite, Fracture process zone, Mixed mode I/II loading.

**Nomenclature**

FPZ	Fracture process zone
SED	Strain energy density
MTS	Maximum tangential stress
SER	Strain energy release
MSS	Maximum shear stress
SIF	Stress intensity factor
DCB	Double cantilever beam
MMB	Mixed mode bending
ENF	End notched flexure
$w$	Strain energy density function
$w_c$	Critical strain energy density
$w_{FPZ}$	Strain energy density of fracture process zone
$w_{FPZ_I}, w_{FPZ_{II}}$	Strain energy density of FPZ under pure mode I and pure mode II
$W$	Strain energy
$\sigma_{ij}$	Stress field around the crack tip
$\varepsilon_{ij}$	Strain field around the crack tip
$K_I, K_{II}$	Mode I and mode II stress intensity factor
$K_{Ic}, K_{IIc}$	Mode I and mode II fracture toughness
$K_{FPZ_I}, K_{FPZ_{II}}$	Stress intensity factor of FPZ under pure mode I and pure mode II
$r$	Distance from the crack tip
$\theta$	Angle from the crack tip
$\theta_0$	Crack initiation angle
$\theta_{0_I}, \theta_{0_{II}}$	Crack initiation angle under mode I and mode II loading
$C_{ij}$	Components of compliance matrix for the plane stress conditions
$C'_{ij}$	Components of compliance matrix for the plane strain conditions
$S$	Strain energy density factor
$S_{cr}$	Critical strain energy density factor
$\rho$	Damage factor
$\rho'$	Modified damage factor
$\rho''$	Toughening damage factor
$\rho_{FPZ}$	FPZ damage factor

$\alpha_i, \quad i = 1, 2, 3$	Inverse of defined damage factors
$G$	Strain energy release rate
$G_{FPZ}$	Energy absorbed by the fracture process zone
$G_{FPZ_I}, G_{FPZ_{II}}$	Absorbed energy of FPZ under pure mode I and pure mode II
$G_{Pe}$	Energy absorbed by the fiber peel-off
$G_{Debonding}$	Energy absorbed by the fiber-matrix debonding
$G_n, G_t$	Normal and tangential components of energy contribution of bridging fiber analyzed as a beam
$E'_I, E'_{II}$	Generalized elastic moduli
$L_{Pe}$	Fiber peel-off length
$d$	Fiber diameter
$E_f$	Young's modulus of the fiber
$L_{Pu}$	Fiber pull-out length
$L_d$	Length of debonding zone
$\sigma_{bf}$	Fiber tensile strength
$\delta_n, \delta_t$	Normal and tangential crack opening displacement
$T_n, T_t$	Normal and tangential traction of the bridging zone
$f_n, f_t$	Force per fiber in normal and tangential directions
$n_0$	Initial number of bridging fibers per unit area
$n$	Number of bridging fibers per unit area
$a$	Dimensionless coefficient
$l_0$	Initial bridging length
$\tau_i$	Interface frictional shear resistance
$A_f$	The cross-sectional area of the bridging fiber
$\varphi$	The angle between the bridging fiber and crack surface
$\sigma_{ref}$	Weibull reference strength
$l_{ref}$	Weibull reference length
$m$	Weibull modulus of the fiber
$c_b$	Dimensionless correction factor
$\bar{\sigma}$	Stress in the bridging fiber
$G_{ic}$	Interfacial debonding energy
$E_i, \quad i = 1, 2, 3$	Young's moduli in the $i$ direction
$L, R, T$	Wood Longitudinal, Radial, Tangential direction
$G_{ij}$	Shear modulus
$\nu_{ij}$	Poisson's ratio

## 1. Introduction

Delamination is one of the most important failure modes in laminated composites and commonly happens under mixed mode I/II loading. The quasi-brittle delamination failure of orthotropic composite materials is generally associated with the creation of a fracture process zone (FPZ) around the delamination tip. This zone contains toughening mechanisms such as fiber bridging and micro-cracking that delay the fracture phenomenon by the energy absorption [1-3]. Therefore, a failure criterion, capable of considering the fracture process zone effects, presents a more accurate estimation of the failure in orthotropic composite materials. Various failure criteria [4-6] are available for predicting delamination growth in laminated composites under the mixed mode I/II loading. The delamination behavior of laminated composites is a complex phenomenon due to the formation of FPZ at the crack tip, especially in the mixed mode I/II loading. Due to these complications, the first criteria presented in this field were based on curve fitting of experimental data [7-10]. Most of these empirical criteria are old, and there is some material constant in these criteria that must be obtained by experiments for each crack configuration.

Another approach has been used by some researchers to present a suitable orthotropic mixed mode I/II failure criterion by extending the well-known isotropic fracture theories to orthotropic materials. Jernkvist in 2001 [11] extended several available isotropic fracture theories, namely maximum strain energy release rate (SER) [12], minimum strain energy density (SED) and maximum tangential stress (MTS) theories [13], to develop mixed mode I/II failure criteria for prediction of the mixed mode I/II fracture of wood specimens as orthotropic materials. The introduced criteria by Jernkvist were so conservative and the extracted results were not consistent with experimental data [15]. This incompatibility is attributed to linear assumptions during the

fracture analysis and ignoring the absorbed energy by toughening mechanisms such as micro-cracks formation in FPZ. In 2013, Fakoor et al. [16] extended the maximum shear stress (MSS) criterion to orthotropic materials, which resulted in the well-known 'Wu' criterion presented for mixed-mode fracture prediction in orthotropic materials.

The FPZ effects have not been sufficiently considered in the available mixed-mode I/II failure criteria. Some other research has considered the effects of FPZ through a damage factor. Romanowicz et al. in 2008 [17] correctly understood that the FPZ has an important role in failure process of orthotropic materials. They proposed a mixed mode I/II failure criterion employing a non-local stress fracture criterion to orthotropic materials based on the damage model of an elastic solid containing growing micro-cracks. By defining a damage factor in their model, the effect of FPZ was considered. But, because of the dependence of this factor on complicated parameters such as the micro-crack density and the actual micro-crack size, they could not calculate the proposed damage factor appropriately. In 2010, Anaraki et al. [18] proposed a general mixed mode I/II failure criterion applicable to orthotropic materials considering a damage factor for FPZ based on calculated damage properties for an elastic solid containing randomly distributed micro-cracks. Also, they calculated the introduced damage factor using strength properties of orthotropic materials along and perpendicular to fibers with a combination of micro- and macro-approaches in another research [19]. Their approach in calculating the damage parameter was completely theoretical and was not supported by any experimental evidence. Recently, Fakoor et al. [20] extended the concept of the damage factor employing a micromechanical approach together with experimental tests.

As it can be found out from the above literature review, an efficient mixed mode I/II failure criterion that can properly consider the effects of FPZ and related toughening mechanisms has not

been developed yet. Nearly all research conducted so far, has focused on the effects of the micro-cracks formation in the FPZ by defining a damage factor based on the properties of this zone. Despite the fiber bridging as a toughening mechanism plays a significant role in delamination failure of laminated composites, but till now in the proposed criteria, the fiber bridging effects have not been taken into account.

The main objective of the present study is to propose a mixed mode I/II failure criterion to consider effects of energy absorbed in the FPZ due to the formation of toughening mechanisms, such as fiber bridging and micro-cracking. In the present work, the minimum strain energy density theory available for isotropic materials [13, 14] was extended to orthotropic materials and modified in two steps. First, the crack initiation angles under mode I and mode II loading were calculated different from zero. The second modification was done by adding a term of the strain energy density of FPZ to the equations for considering the effects of this zone. According to this approach, a new mixed mode I/II failure criterion expressed in terms of the mixed mode stress intensity factors for orthotropic materials is proposed. This new criterion takes into account the effects of absorbed energy in the FPZ by defining a suitable damage factor. Implementation of the proposed criterion for prediction of mixed mode I/II crack growth is straightforwardly possible by considering the mode I fracture toughness, elastic properties of the material and the energy absorbed by the FPZ. This absorbed energy is obtained from the mixed mode I/II micromechanical bridging model based on breakdown of the failure micro-mechanisms involved in the fiber bridging phenomenon. Some verifications have been done with several available experimental data for both laminated composites and wood species.

## **2. Theoretical background**

In order to derive a mixed mode I/II failure criterion for orthotropic materials we first briefly review the minimum strain energy density theory of this kind of materials. Sih [13] has proposed a fracture theory based on the local strain energy density at the crack tip. Consider a structure with a through-crack that extends on the  $x_1$ - $x_3$  plane in a linear-elastic orthotropic material. In this case, the strain energy stored in a volume element  $dV$  is defined as the strain energy density,  $w$ , around the crack tip:

$$w = \frac{dW}{dV} = \frac{1}{2} \sigma_{ij} \varepsilon_{ij} \quad (1)$$

The stress field around the crack tip of an orthotropic cracked body is given by [21]:

$$\sigma_{ij} = \frac{1}{\sqrt{2\pi r}} (K_I f_{ij}(\theta) + K_{II} g_{ij}(\theta)), \quad (i, j = 1, 2) \quad (2)$$

where the polar components  $r$  and  $\theta$  are defined in Fig. 1, and the angular functions  $f_{ij}(\theta)$  and  $g_{ij}(\theta)$  depend on the plane strain constitutive matrix and defined in [21] as follows:

$$\begin{aligned} f_{11}(\theta) &= \operatorname{Re} \left[ \frac{x_1 x_2 (x_2 F_2 - x_1 F_1)}{x_1 - x_2} \right], & g_{11}(\theta) &= \operatorname{Re} \left[ \frac{x_2^2 F_2 - x_1^2 F_1}{x_1 - x_2} \right] \\ f_{22}(\theta) &= \operatorname{Re} \left[ \frac{x_1 F_2 - x_2 F_1}{x_1 - x_2} \right], & g_{22}(\theta) &= \operatorname{Re} \left[ \frac{F_2 - F_1}{x_1 - x_2} \right] \\ f_{12}(\theta) &= \operatorname{Re} \left[ \frac{x_1 x_2 (F_1 - F_2)}{x_1 - x_2} \right], & g_{12}(\theta) &= \operatorname{Re} \left[ \frac{x_1 F_1 - x_2 F_2}{x_1 - x_2} \right] \end{aligned} \quad (3)$$

where

$$F_1 = \frac{1}{(\cos\theta + x_1 \sin\theta)^{\frac{1}{2}}}, \quad F_2 = \frac{1}{(\cos\theta + x_2 \sin\theta)^{\frac{1}{2}}} \quad (4)$$

$x_1$  and  $x_2$  are the conjugate pair of roots of the following characteristic equation.

$$C_{11} x^4 - 2C_{16} x^3 + (2C_{12} + C_{66}) x^2 - 2C_{26} x + C_{22} = 0 \quad (5)$$

where the coefficients  $C_{ij}$  are derived from the following material constitutive relation

( $\varepsilon_i = C_{ij}\sigma_j$ ):

$$\begin{pmatrix} \varepsilon_{11} \\ \varepsilon_{22} \\ \varepsilon_{33} \\ \gamma_{23} \\ \gamma_{31} \\ \gamma_{12} \end{pmatrix} = \begin{pmatrix} 1/E_1 & -\nu_{21}/E_2 & -\nu_{31}/E_3 & 0 & 0 & 0 \\ -\nu_{12}/E_1 & 1/E_2 & -\nu_{32}/E_3 & 0 & 0 & 0 \\ -\nu_{13}/E_1 & -\nu_{23}/E_2 & 1/E_3 & 0 & 0 & 0 \\ 0 & 0 & 0 & 1/G_{23} & 0 & 0 \\ 0 & 0 & 0 & 0 & 1/G_{31} & 0 \\ 0 & 0 & 0 & 0 & 0 & 1/G_{12} \end{pmatrix} \begin{pmatrix} \sigma_{11} \\ \sigma_{22} \\ \sigma_{33} \\ \sigma_{23} \\ \sigma_{31} \\ \sigma_{12} \end{pmatrix} \quad (6)$$

Only five quantities of  $C_{ij}$  ( $C_{11}, C_{22}, C_{12}, C_{21}$  and  $C_{66}$ ) are relevant to the  $x_1$ - $x_2$  plane stress conditions. For the conditions of plane strain, four of the in-plane compliances need to be replaced by  $C'_{ij}$  that can be related to  $C_{ij}$  as follows:

$$C'_{ij} = C_{ij} - \frac{C_{i3}C_{j3}}{C_{33}}, \quad (i, j = 1, 2) \quad (7)$$

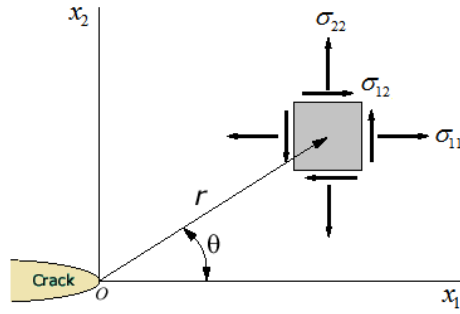


**Fig. 1. Stress components around the crack tip of a cracked body.**

Under plane strain conditions, substituting Eq. (6) into Eq. (1) yields the following form for the strain energy density:

$$w = \frac{C'_{11}}{2} \sigma_{11}^2 + \frac{C'_{22}}{2} \sigma_{22}^2 + C'_{12} \sigma_{11} \sigma_{22} + \frac{C'_{66}}{2} \sigma_{12}^2 \quad (8)$$

By substitution of the crack tip singular stress state from Eq. (2) into Eq. (8):

$$w = K_I^2 A_1(\theta) + K_{II}^2 A_2(\theta) + 2K_I K_{II} A_3(\theta) \quad (9)$$

where the coefficients  $A_i$ , for  $i = 1, 2$  and  $3$ , are complicated functions of the orthotropic material constants and depend on the angle  $\theta$  and defined by:

$$\begin{aligned} A_1(\theta) &= \left[ \frac{C'_{11}}{4\pi r} f_{11}^2(\theta) + \frac{C'_{22}}{4\pi r} f_{22}^2(\theta) + \frac{C'_{12}}{2\pi r} f_{11}(\theta) f_{22}(\theta) + \frac{C'_{66}}{4\pi r} f_{12}^2(\theta) \right] \\ A_2(\theta) &= \left[ \frac{C'_{11}}{4\pi r} g_{11}^2(\theta) + \frac{C'_{22}}{4\pi r} g_{22}^2(\theta) + \frac{C'_{12}}{2\pi r} g_{11}(\theta) g_{22}(\theta) + \frac{C'_{66}}{4\pi r} g_{12}^2(\theta) \right] + \\ A_3(\theta) &= \left[ \frac{C'_{11}}{4\pi r} f_{11}(\theta) g_{11}(\theta) + \frac{C'_{22}}{4\pi r} f_{22}(\theta) g_{22}(\theta) + \frac{C'_{12}}{4\pi r} (f_{11}(\theta) g_{22}(\theta) + f_{22}(\theta) g_{11}(\theta)) \right] \end{aligned} \quad (10)$$

Hence, the amplitude or the intensity of the strain energy density field, namely strain energy density factor,  $S$ , is given by:

$$w = \frac{dW}{dV} = \frac{S}{r} \quad \longrightarrow \quad S = K_I^2 D_1(\theta) + K_{II}^2 D_2(\theta) + 2K_I K_{II} D_3(\theta) \quad (11)$$

where coefficients  $D_i(\theta) = rA_i(\theta)$ . The minimum strain energy density theory states that:

- (1) Crack initiation occurs in a direction determined by the minimum strain energy density factor:

$$\frac{\partial S}{\partial \theta} = 0 \quad \text{and} \quad \frac{\partial^2 S}{\partial \theta^2} > 0 \quad \text{at} \quad \theta = \theta_0 \quad (12)$$

- (2) Crack growth occurs when the minimum strain energy density factor reaches its critical value:

$$S_{\min} = S_{cr} \quad \text{at} \quad \theta = \theta_0 \quad (13)$$

### 3. Derivation of failure criterion

The mixed mode I/II failure criterion proposed by Jernkvist [11] was based on a general simplifying assumption that the crack propagation direction in wood components is along the fibers ( $\theta_0 = 0$ ), under any of the loading modes. In his analysis, it was also assumed that the critical strain energy density,  $w_c$ , can be used as an intrinsic material parameter whose value is independent of the degree of mode mixity. So, all differences between the toughening mechanisms of FPZ under mode I and mode II are ignored. By extending the minimum strain energy density theory to wooden structures as orthotropic materials together with these simplifying assumptions, he derived a mixed mode I/II failure criterion in terms of the stress intensity factors as follows [11]:

$$K_I^2 + \rho K_{II}^2 = K_{Ic}^2 \quad (14)$$

in which,  $\rho$  is a damage factor and given by:

$$\rho = \frac{1}{\alpha_1} = \left[ \frac{C'_{66} g_{12}^2(0)}{C'_{11} f_{11}^2(0) + C'_{22} f_{22}^2(0) + 2C'_{12} f_{11}(0) f_{22}(0)} \right] \quad (15)$$

The critical strain energy density approach can be used in order to investigate the delamination failure in orthotropic laminated composites. Unlike isotropic materials, in composite materials the crack initiation angle  $\theta_0$  is different from zero even under pure mode I loading [22]. So, in order to propose a mixed mode I/II failure criterion for prediction of the delamination growth in laminated composites, the criterion in Eqs. (14) and (15) has been modified in the following. An example of the initial crack initiation angle in delamination of a glass/epoxy laminated composite under pure mode I, mixed mode I/II (50%) and pure mode II is shown in Fig. (2). The photographs in Fig. (2) were obtained from double cantilever beam (DCB), mixed mode bending (MMB) and end notched flexure (ENF) tests performed by the authors and will be fully described in another publication.

**Met opmerkingen [RA-L1]:** Is it loading mode, or an opening mode?

It is any of the loading modes because Jernkvist in his work assumed that the crack propagation direction in wood is given by the fiber direction (theta=0), independent of the loading mode.

**Met opmerkingen [RA-L2]:** Why the '(0)' in the eq?

Jernkvist assumed that the crack propagation direction is along the wood fibers (theta=0). So, theta equal to zero is substituted in the related equations.

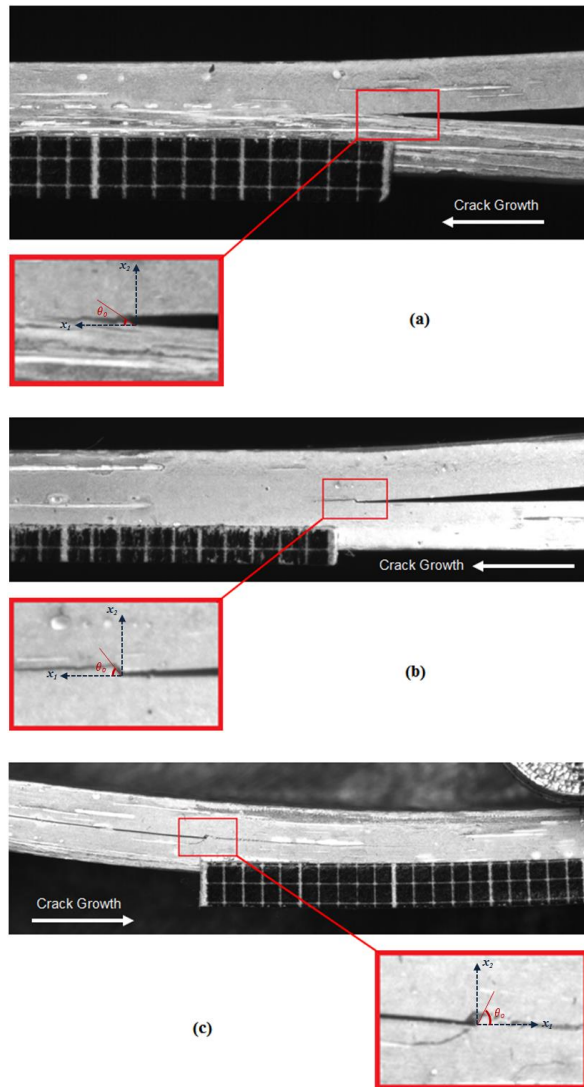


**Fig. 2. Crack initiation angle in delamination of a glass/epoxy laminated composite under (a) Pure mode I, (b) Mixed mode I/II (50%) and (c) Pure mode II. The tests were performed by the authors.**

Consider a failure criterion as follows:

$$w = K_I^2 A_1(\theta_0) + K_{II}^2 A_2(\theta_0) + 2K_I K_{II} A_3(\theta_0) = w_c \quad (16)$$

For the cases of the pure mode I and pure mode II, Eq. (16) is in the following simple forms:

$$\begin{aligned} \xrightarrow{\text{Pure Mode I}} \quad w_I &= A_1(\theta_{0_I}) K_{Ic}^2 = w_c \\ \xrightarrow{\text{Pure Mode II}} \quad w_{II} &= A_2(\theta_{0_{II}}) K_{IIc}^2 = w_c \end{aligned} \quad (17)$$

where  $\theta_{0_I}$  and  $\theta_{0_{II}}$  are the crack initiation angle under mode I and mode II loading. In this analysis, the critical strain energy density is still considered as a material parameter, independent of the loading mode. Since the criterion in Eq. (16) should be applicable for both pure mode I and pure mode II loading, we have:

$$\frac{K_{IIc}^2}{K_{Ic}^2} = \frac{A_1(\theta_{0_I})}{A_2(\theta_{0_{II}})} = \alpha_2 \quad (18)$$

Using this relation in Eq. (16), a mixed mode failure criterion in terms of stress intensity factors can be expressed as:

$$K_I^2 + \rho' K_{II}^2 = K_{Ic}^2 \quad (19)$$

where  $\rho'$  as a “modified damage factor” is defined by:

$$\rho' = \frac{1}{\alpha_2} = \frac{A_2(\theta_{0_{II}})}{A_1(\theta_{0_I})} = \left[ \frac{C'_{11} g_{11}^2(\theta_{0_{II}}) + C'_{22} g_{22}^2(\theta_{0_{II}}) + 2C'_{12} g_{11}(\theta_{0_{II}}) g_{22}(\theta_{0_{II}}) + C'_{66} g_{12}^2(\theta_{0_{II}})}{C'_{11} f_{11}^2(\theta_{0_I}) + C'_{22} f_{22}^2(\theta_{0_I}) + 2C'_{12} f_{11}(\theta_{0_I}) f_{22}(\theta_{0_I}) + C'_{66} f_{12}^2(\theta_{0_I})} \right] \quad (20)$$

It can be seen that Eq. (20), in the case of  $\theta_0 = \theta_{0_I} = \theta_{0_{II}} = 0$ , reduces to Eq. (15) which has been proposed by Jernkvist [11]. For determination of  $\rho'$ , we need to calculate the values of the crack initiation angles under pure mode I and pure mode II,  $\theta_{0_I}$  and  $\theta_{0_{II}}$ . To this end, consider the delamination under pure mode I and pure mode II loading in a linear-elastic orthotropic composite laminate. Using Eq. (11), the strain energy density factors for the pure mode I and II are given by:

$$\begin{aligned}
\text{Pure Mode I} &\rightarrow S_I = K_I^2 D_1(\theta) \\
\text{Pure Mode II} &\rightarrow S_{II} = K_{II}^2 D_2(\theta)
\end{aligned} \tag{21}$$

Applying conditions expressed in Eq. (12) to Eq. (21), we have:

$$\begin{aligned}
\text{Pure Mode I} &\rightarrow \frac{\partial D_1(\theta)}{\partial \theta} = 0, \quad \frac{\partial^2 D_1(\theta)}{\partial \theta^2} > 0 \quad \text{at } \theta = \theta_{0_I} \\
\text{Pure Mode II} &\rightarrow \frac{\partial D_2(\theta)}{\partial \theta} = 0, \quad \frac{\partial^2 D_2(\theta)}{\partial \theta^2} > 0 \quad \text{at } \theta = \theta_{0_{II}}
\end{aligned} \tag{22}$$

where

$$\begin{aligned}
\frac{\partial D_1(\theta)}{\partial \theta} &= \frac{1}{2\pi} [C'_{11} f_{11}(\theta) \frac{\partial f_{11}(\theta)}{\partial \theta} + C'_{22} f_{22}(\theta) \frac{\partial f_{22}(\theta)}{\partial \theta} + C'_{12} (\frac{\partial f_{11}(\theta)}{\partial \theta} f_{22}(\theta) + f_{11}(\theta) \frac{\partial f_{22}(\theta)}{\partial \theta}) + C'_{66} f_{12}(\theta) \frac{\partial f_{12}(\theta)}{\partial \theta}] \\
\frac{\partial D_2(\theta)}{\partial \theta} &= \frac{1}{2\pi} [C'_{11} g_{11}(\theta) \frac{\partial g_{11}(\theta)}{\partial \theta} + C'_{22} g_{22}(\theta) \frac{\partial g_{22}(\theta)}{\partial \theta} + C'_{12} (\frac{\partial g_{11}(\theta)}{\partial \theta} g_{22}(\theta) + g_{11}(\theta) \frac{\partial g_{22}(\theta)}{\partial \theta}) + C'_{66} g_{12}(\theta) \frac{\partial g_{12}(\theta)}{\partial \theta}]
\end{aligned} \tag{23}$$

and

$$\begin{aligned}
\frac{\partial^2 D_1(\theta)}{\partial \theta^2} &= \frac{1}{2\pi} [C'_{11} ((\frac{\partial f_{11}(\theta)}{\partial \theta})^2 + f_{11}(\theta) \frac{\partial^2 f_{11}(\theta)}{\partial \theta^2}) + C'_{22} ((\frac{\partial f_{22}(\theta)}{\partial \theta})^2 + f_{22}(\theta) \frac{\partial^2 f_{22}(\theta)}{\partial \theta^2}) + \\
&\quad C'_{12} (\frac{\partial^2 f_{11}(\theta)}{\partial \theta^2} f_{22}(\theta) + 2 \frac{\partial f_{11}(\theta)}{\partial \theta} \frac{\partial f_{22}(\theta)}{\partial \theta} + f_{11}(\theta) \frac{\partial^2 f_{22}(\theta)}{\partial \theta^2}) + C'_{66} ((\frac{\partial f_{12}(\theta)}{\partial \theta})^2 + f_{12}(\theta) \frac{\partial^2 f_{12}(\theta)}{\partial \theta^2})] \\
\frac{\partial^2 D_2(\theta)}{\partial \theta^2} &= \frac{1}{2\pi} [C'_{11} ((\frac{\partial g_{11}(\theta)}{\partial \theta})^2 + g_{11}(\theta) \frac{\partial^2 g_{11}(\theta)}{\partial \theta^2}) + C'_{22} ((\frac{\partial g_{22}(\theta)}{\partial \theta})^2 + g_{22}(\theta) \frac{\partial^2 g_{22}(\theta)}{\partial \theta^2}) + \\
&\quad C'_{12} (\frac{\partial^2 g_{11}(\theta)}{\partial \theta^2} g_{22}(\theta) + 2 \frac{\partial g_{11}(\theta)}{\partial \theta} \frac{\partial g_{22}(\theta)}{\partial \theta} + g_{11}(\theta) \frac{\partial^2 g_{22}(\theta)}{\partial \theta^2}) + C'_{66} ((\frac{\partial g_{12}(\theta)}{\partial \theta})^2 + g_{12}(\theta) \frac{\partial^2 g_{12}(\theta)}{\partial \theta^2})]
\end{aligned} \tag{24}$$

Since above equations are non-linear and complex, it is too difficult to obtain  $\theta_{0_I}$  and  $\theta_{0_{II}}$

theoretically. This is one of the reasons that Jernkvist assumed the crack propagation direction is followed by the fiber direction [11]. In the present research, solving the resulting equations (Eqs. (22-24)) numerically for the given material properties, it is found that the angle in which the function  $D_1$  reaches its minimum is the angle predicted for the first crack propagation under pure mode I delamination ( $\theta_{0_I}$ ). Similarly, the angle in which the function  $D_2$  achieves its minimum value is the angle predicted for the first crack propagation under pure mode II delamination ( $\theta_{0_{II}}$ ).

The delamination failure phenomenon in laminated composites is accompanied by the formation of the FPZ at the crack tip. There are several toughening mechanisms in this zone that delay the

fracture by absorbing energy. The activation of these mechanisms and the extent of their effects depend on the loading mode. For example, fiber bridging which is often activated by the presence of mode I loading is more effective in predominantly mode I than the micro-cracking which is often due to the presence of mode II loading and therefore more effective in predominantly mode II [23]. Photographs and schematic of fracture process zone with related toughening mechanisms in delamination of laminated composites are presented in Fig. 3. The photographs in Fig. 3 were obtained from mixed mode bending (MMB) test performed by the authors and its results will be fully discussed in another publication.

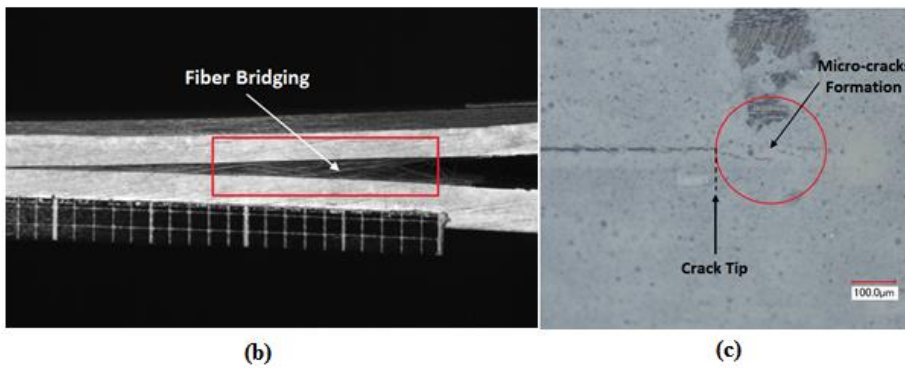
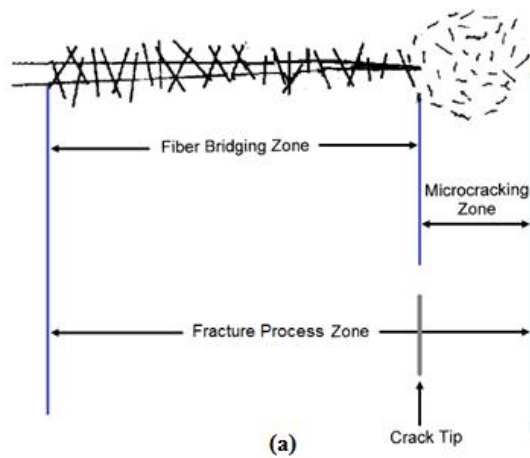


**Fig. 3. (a) Schematic of fracture process zone in laminated composites; (b) Photograph of fiber bridging behind the crack tip and (c) Optical micrograph of the micro-cracks formation around the crack tip. The test was performed by the authors.**

As previously stated, assuming the critical strain energy density,  $w_c$ , as a material property and independent of the loading mode, all differences between the effects of FPZ under mode I and mode II are neglected. So, to consider FPZ effects and consequently a more precise prediction of delamination failure in laminated composites, the failure criterion in Eq. (16) is modified by adding the term of the strain energy density of FPZ,  $w_{FPZ}$ , as follows:

$$w = K_I^2 A_1(\theta_0) + K_{II}^2 A_2(\theta_0) + 2K_I K_{II} A_3(\theta_0) = w_c + w_{FPZ} \quad (25)$$

For the cases of pure mode I and pure mode II loading, we have:

$$\begin{aligned} \xrightarrow{\text{Pure Mode I}} \quad w_I &= A_1(\theta_{0_I}) K_{Ic}^2 = w_c + w_{FPZ_I} \\ \xrightarrow{\text{Pure Mode II}} \quad w_{II} &= A_2(\theta_{0_{II}}) K_{IIc}^2 = w_c + w_{FPZ_{II}} \end{aligned} \quad (26)$$

where  $w_{FPZ_I}$  and  $w_{FPZ_{II}}$  are the strain energy density of FPZ under pure mode I and pure mode II loading, respectively and defined by:

$$\begin{aligned} w_{FPZ_I} &= A_1(\theta_{0_I}) K_{FPZ_I}^2 \\ w_{FPZ_{II}} &= A_2(\theta_{0_{II}}) K_{FPZ_{II}}^2 \end{aligned} \quad (27)$$

where  $K_{FPZ_I}$  and  $K_{FPZ_{II}}$  are introduced as mode I and II stress intensity factors (SIFs) of FPZ, respectively. Using the relation between SIFs and the strain energy release rate ( $G$ ) for orthotropic materials under plane strain condition [21], we have:

$$\begin{aligned} K_{FPZ_I} &= \sqrt{E'_I G_{FPZ_I}} \\ K_{FPZ_{II}} &= \sqrt{E'_{II} G_{FPZ_{II}}} \end{aligned} \quad (28)$$

**Met opmerkingen [RA-L3]:** You call in the nomenclature these  $G$ 's energy absorption, rather than energy release rate. Should you more specifically define your terminology? Is energy release the same as energy absorption? Is this absorption permanent, or do bridging fibre for example release the energy upon unloading? With reference to Yao, shielding technically stores energy, it doesn't release or absorb it...

The energy absorption by FPZ ( $G_{FPZ}$ ) is a part of strain energy release rate at crack propagation ( $G_{ic}$ ). As you know,  $G_{ic}$  is equal to summation of strain energy release rate at crack initiation ( $G_i$ ) and  $G_{FPZ}$ .

Energy of the FPZ has been called the absorbed energy by the toughening mechanisms (fiber bridging and micro-cracking) that is released by crack growth. It just means that the toughening mechanisms are as a absorption storage of energy and delay the fracture by consuming (releasing) more energy for crack growth.

where  $E'_I$  and  $E'_{II}$  are generalized elastic moduli [21] and defined as:

$$\begin{aligned} E'_I &= \left[ \frac{C'_{11}C'_{22}}{2} \left( \sqrt{\frac{C'_{22}}{C'_{11}}} + \frac{2C'_{12} + C'_{66}}{2C'_{11}} \right) \right]^{-1} \\ E'_{II} &= \left[ \frac{C'^2_{11}}{2} \left( \sqrt{\frac{C'_{22}}{C'_{11}}} + \frac{2C'_{12} + C'_{66}}{2C'_{11}} \right) \right]^{-1} \end{aligned} \quad (29)$$

It should be noted that coefficients  $A_1$  and  $A_2$  in Eq. (27) and  $E'_I$  and  $E'_{II}$  in Eq. (28) should be expressed in terms of the effective elastic properties of the FPZ as a damaged zone [20, 24, 25]. However, in the present study, we considered them equal to properties of the intact material, as a simplifying assumption. This part of the theory/criterion can be improved in the future works.

Substituting Eq. (27) into Eq. (26) and considering that the criterion in Eq. (25) should be applicable to the pure mode I and pure mode II loading, we find:

$$\frac{K^2_{IIc}}{K^2_{Ic}} = \frac{A_1(\theta_{0_I})}{A_2(\theta_{0_{II}})} - \frac{A_1(\theta_{0_I})}{A_2(\theta_{0_{II}})} \left( \frac{K_{FPZ_I}}{K_{Ic}} \right)^2 + \left( \frac{K_{FPZ_{II}}}{K_{Ic}} \right)^2 = \alpha_3 \quad (30)$$

Applying this relation in Eq. (25) yields a new mixed mode I/II failure criterion expressed in the form of common mixed-mode failure criterion as follows:

$$K_I^2 + \rho'' K_{II}^2 = K_{Ic}^2 \quad (31)$$

where  $\rho''$  is introduced as a ‘‘toughening damage factor’’ as follows:

$$\rho'' = \frac{1}{\alpha_3} \quad \longrightarrow \quad \frac{1}{\rho''} = \frac{1}{\rho'} + \frac{1}{\rho_{FPZ}} \quad (32)$$

The proposed toughening damage factor,  $\rho''$ , includes both the orthotropic damage factor,  $\rho'$ , given in Eq. (20) and the FPZ damage factor,  $\rho_{FPZ}$ , defined as:

$$\rho_{FPZ} = \frac{1}{\left(-\frac{A_1(\theta_{0_I})}{A_2(\theta_{0_{II}})}\left(\frac{K_{FPZ_I}}{K_{Ic}}\right)^2 + \left(\frac{K_{FPZ_{II}}}{K_{Ic}}\right)^2\right)} \quad (33)$$

Eq. (31) shows a simple mixed mode I/II failure criterion in terms of stress intensity factors  $K_I$  and  $K_{II}$  with two material parameters ( $K_{Ic}$  and  $\rho''$ ). The first parameter, namely the mode I fracture toughness, can be simply extracted from available experimental data [8, 9, 15]. The second one is a toughening damage factor, demonstrating the toughening effects of the FPZ in the delamination tip vicinity due to the fiber bridging and micro-cracks formation. Damage factor  $\rho''$ , depends on  $K_{Ic}$ ,  $\theta_{0_I}$ ,  $\theta_{0_{II}}$ ,  $A_1$ ,  $A_2$ ,  $K_{FPZ_I}$  and  $K_{FPZ_{II}}$  parameters. Wherein the crack initiation angles under pure mode I and pure mode II ( $\theta_{0_I}$  and  $\theta_{0_{II}}$ ) are calculated by Eq.(22). The coefficients  $A_1$  and  $A_2$  are obtained using Eq.(10) having material properties and crack initiation angles. According to Eq. (28), in order to calculate the mode I and II stress intensity factors of FPZ ( $K_{FPZ_I}$  and  $K_{FPZ_{II}}$ ), the absorbed energy of FPZ under pure mode I and pure mode II loading is needed. This approach is briefly discussed in the following section.

#### 4. Calculation of the absorbed energy by the FPZ ( $G_{FPZ}$ )

In delamination of unidirectional laminated composites, fiber bridging is known as the most important toughening mechanism absorbing the highest amount of energy in the FPZ. The absorbed energy by the fiber bridging toughening mechanism in FPZ is often calculated by bridging laws [26, 27]. The bridging laws are defined as a relationship between bridging tractions and crack separations. Bridging laws can be extracted from experiments or micromechanical models.

It is well-known that the "crack growth resistance curve" or R-curve, shown in Fig. 4, is an

**Met opmerkingen [RA-L4]:** Please don't refer to these as 'laws', they're certainly not laws, but mostly empirical relations. Exactly, that's right but in nearly all research studies, the relationship between bridging tractions and crack separations has been called bridging laws or traction-separation laws. I am so thankful if you let me know your suggested word instead of 'laws' here.

appropriate method for quantifying the FPZ effects. The bridging law can be experimentally determined by measuring the end-opening displacement of the bridging zone together with the R-curve [28, 29].

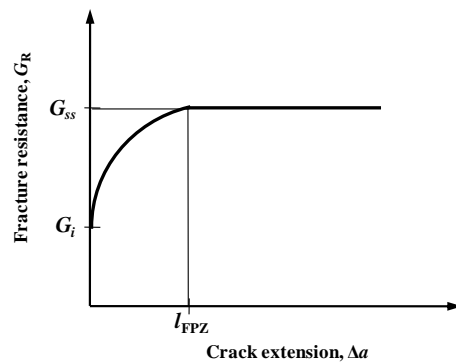


Fig. 4. R-curve for delamination failure in a laminated composite.

Furthermore, there is a number of micromechanical models [30, 31] developed to investigate the delamination by considering fiber bridging effects. Sørensen et al. [32] proposed a micromechanical model for prediction of the mixed mode I/II bridging laws based on the observed bridging mechanism during crack growth in a unidirectional carbon/epoxy composite. In their model, it was assumed that the number of bridging fibers per unit crack area is constant. While the number of fiber failures is negligible until bending stress at the fiber roots does not exceed the mean fiber strength. The bridging fibers start to fail by increasing the bending stress at fiber roots, which means that the number of bridging fibers decreases due to the fiber failure [31]. Daneshjoo et al. [33] developed a mixed mode I/II micromechanical bridging model based on the breakdown of the failure micro-mechanisms involved during the fiber bridging phenomenon such as the fiber

**Met opmerkingen [RA-L5]:** Does this graph apply to all modes? Or just to mode I? Is the resistance curve increasing through development of bridging fibres, or does the micro-cracking in Mode II do the same?  
**No, that's not the same. This figure schematically shows an example of R-curve for delamination failure in a laminated composite.**

peel-off, matrix spalling, fiber-matrix debonding, fiber pull-out and fiber fracture. In their model, the bridging fiber was analyzed as a beam under different loading conditions and the energy absorption of the fiber bridging in FPZ was obtained as [33]:

$$\begin{aligned}
 G_{FPZ} &= G_{FPZ_I} + G_{FPZ_{II}} = \\
 &= (G_n + G_{Pe}) + (G_t + G_{debonding}) = \\
 &= \left( \int_0^{\delta_n^{\max}} T_n(\delta) d\delta_n + G_{Pe} \right) + \left( \int_0^{\delta_t^{\max}} T_t(\delta) d\delta_t + G_{debonding} \right)
 \end{aligned} \quad (34)$$

in which  $G_{Pe}$  was defined as the energy absorption of the fiber peel-off and given by [33, 34]:

$$G_{Pe} = n_0 \frac{\pi d^2 \sigma_{bf}^2}{12 E_f} L_{Pe} \quad (35)$$

where  $n_0$  is the initial number of bridging fibers per unit crack area,  $d$  is the fiber diameter,  $\sigma_{bf}$  is the fiber tensile strength,  $E_f$  is Young's modulus of the fiber and  $L_{Pe}$  is the fiber peel-off length. For calculation of the energy contribution of bridging fibers,  $G_n$  and  $G_t$ , the normal and tangential tractions of the bridging fiber ( $T_n(\delta_n, \delta_t)$  and  $T_t(\delta_n, \delta_t)$ ) are dependent on the force per fiber in the normal and tangential directions ( $f_n(\delta_n, \delta_t)$  and  $f_t(\delta_n, \delta_t)$ ) and the number of bridging fibers per unit crack area ( $n(\delta_n, \delta_t)$ ) as follows [33]:

$$\begin{aligned}
 T_n(\delta_n, \delta_t) &= n(\delta_n, \delta_t) f_n(\delta_n, \delta_t) \\
 T_t(\delta_n, \delta_t) &= \frac{n(\delta_n, \delta_t)}{a} f_t(\delta_n, \delta_t), \quad a > 1
 \end{aligned} \quad (36)$$

where  $\delta_n$  and  $\delta_t$  are the normal and tangential crack opening displacements,  $a$  is a dimensionless coefficient, demonstrating only  $1/a$  number of bridging fibers are involved in the tangential load transfer. Considering the stress in the bridging fiber and the stress reduction due to fiber slip, the normal and tangential components of the force carried by each of bridging fiber were obtained as [33]:

$$\begin{aligned}
f_n(\delta_n, \delta_t) &= A_f \cdot \left[ \frac{E_f \tan^2 \varphi}{16 \left(\frac{c}{d}\right)^2} \cdot \left(\frac{\delta_n}{l_0 + \delta_t}\right) + \sqrt{\frac{2\tau_i E_f l_0}{d}} \left(\frac{2\delta_t}{l_0} + \frac{\delta_n^2}{l_0^2}\right)^{1/2} \cdot \left(\frac{\delta_n}{l_0 + \delta_t}\right) \right] \\
f_t(\delta_n, \delta_t) &= A_f \cdot \left[ \frac{E_f \tan^2 \varphi}{16 \left(\frac{c}{d}\right)^2} + \sqrt{\frac{2\tau_i E_f l_0}{d}} \left(\frac{2\delta_t}{l_0} + \frac{\delta_n^2}{l_0^2}\right)^{1/2} \right]
\end{aligned} \tag{37}$$

where  $A_f$ ,  $\varphi$ ,  $l_0$ ,  $\tau_i$  and  $c$  are the cross-sectional area of the bridging fiber, the bridging fiber angle with the crack surface, the initial bridging length, interface frictional shear resistance and the asymptotic distance between the fiber and its axial direction, respectively.

The number of survived bridging fibers was estimated by the Weibull statistical equation [35] as [33]:

$$n(\delta_n, \delta_t) = n_0 \cdot \exp \left[ -c_b \frac{l(\delta_n, \delta_t)}{l_{ref}} \left( \frac{\bar{\sigma}(\delta_n, \delta_t)}{\sigma_{ref}} \right)^m \right] \tag{38}$$

where  $l_{ref}$  and  $\sigma_{ref}$  are the Weibull reference length and the strength, respectively. Moreover,  $m$  is the Weibull modulus and  $C_b$  is a dimensionless correction factor comparing the bending and tensile stresses, and is smaller than 1. Also,  $\bar{\sigma}(\delta_n, \delta_t)$  is the stress in the bridging fiber. The energy contribution of bridging fibers was obtained by substitution of Eqs. (37) and (38) into Eq. (34) and performing an integration [33].

The last term of the energy in Eq. (34) was defined as the energy required for separation of the fiber-matrix interface called the debonding energy ( $G_{Debonding}$ ) and obtained as follows [33]:

$$G_{Debonding} = n_0 \pi d L_d G_{ic} \tag{39}$$

where  $G_{ic}$  is the interfacial debonding energy and  $L_d$  is the length of the debonding zone. Finally, the absorbed energy by fiber bridging in the FPZ was calculated using Eq. (34). More details of

mixed mode I/II micromechanical bridging model are available in [33].

## 5. Results and discussion

### 5.1. Laminated composite materials

Experimental data available in [36] have been used to evaluate the proposed criteria (Eqs. (19) and (31)) in comparison with the classical criterion (Eq. (14)) in which specimens were made of unidirectional E-glass/EPON 826 laminated composites. Table 1 and Table 2 summarize the elastic properties of E-glass/EPON 826 and the necessary parameters for extracting coefficients of the failure criteria, respectively. The coefficients are given in Table 3. The values of  $\theta_{0_I}$  and  $\theta_{0_{II}}$  in Table 2 are calculated by solving Eqs. (22-24). The values of  $G_{FPZ}$  for pure mode I and pure mode II expressed in Table 2 for this kind of material are calculated using the mixed mode I/II micromechanical bridging model briefly described in Section 4. This calculation process is presented in detail in [33].

**Table 1. Elastic properties of E-glass/EPON 826 [37]**

Laminated composite material	$E_1$ (GPa)	$E_2$ (GPa)	$E_3$ (GPa)	$G_{12}$ (GPa)	$G_{13}$ (GPa)	$G_{23}$ (GPa)	$\nu_{12}$	$\nu_{13}$	$\nu_{23}$
E-glass/EPON826	35.25	10.82	10.82	4.28	4.28	3.58	0.27	0.27	0.51

**Table 2. Parameters for extracting coefficients of failure criteria for E-glass/EPON 826**

Laminated composite material	$K_{Ic}$ <sup>a</sup> (MPa.m <sup>0.5</sup> )	$-\theta_{0_I}$ <sup>b</sup> (degree)	$-\theta_{0_{II}}$ <sup>b</sup> (degree)	$G_{FPZ_I}$ <sup>a</sup> (kJ/m <sup>2</sup> )	$G_{FPZ_{II}}$ <sup>a</sup> (kJ/m <sup>2</sup> )
E-glass/EPON826	1.65	31.76	81.27	0.205	2.40

<sup>a</sup> Obtained from Refs. [33, 36].

<sup>b</sup> Calculated in current study.

**Table 3. Dimensionless coefficients in Eqs. (14), (19) and (31) for E-glass/EPON 826**

Laminated composite material	$\rho$	$\rho'$	$\rho''$
E-glass/EPON826	2.326	0.691	0.0517

Fig. 5 shows the mixed mode I/II delamination failure responses predicted by the failure criteria proposed in Section 3. A comparison of the experimental data of E-glass/EPON 826 with the predictions reveals that the newly proposed criterion in Eq. (31) is more compatible with the nature of delamination phenomena in this kind of laminated composite. This compatibility is attributed to the fact that this criterion takes into account the contribution of absorbed energy by fiber bridging in FPZ.

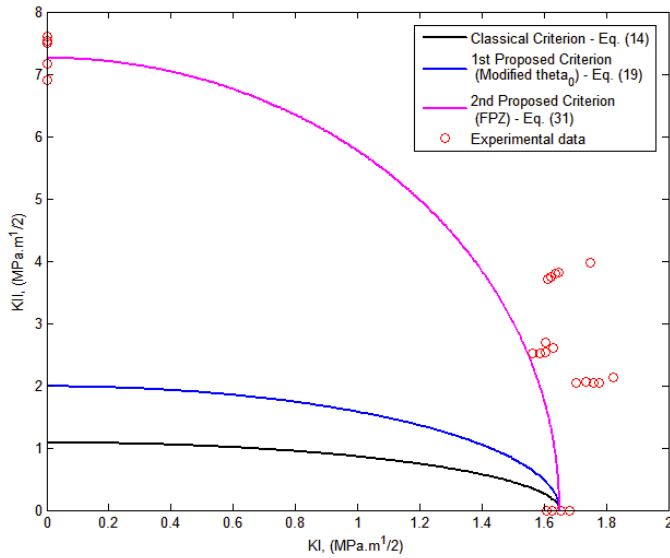


**Fig. 5. Fracture limit curves related to failure criteria in comparison with experimental data [36] for E-glass/EPON 826.**

As can be seen in Fig. 5, the amount of experimental data of E-glass/Epon 826 especially in the case of dominant mode II is not sufficient. So, in order to investigate the validity and accuracy of the newly proposed criteria, experimental mixed mode I/II delamination data of three other laminated composite materials [9] are utilized. The elastic properties of these laminated composites are listed in Table 4. The parameters required for extracting the coefficients of the failure criteria and resulting coefficients are given in Tables 5 and 6, respectively. The values of  $\theta_{0_I}$  and  $\theta_{0_{II}}$  in Table 5 are calculated by solving Eqs. (26-28). In this case, the values of  $G_{FPZ}$  for pure mode I and pure mode II expressed in Table 5 are extracted from the experimental R-curves available in [38-42].

**Table 4. Elastic properties of laminated composite materials used in the analysis [9]**

Laminated composite materials	$E_1$ (GPa)	$E_2$ (GPa)	$E_3$ (GPa)	$G_{12}$ (GPa)	$G_{13}$ (GPa)	$G_{23}$ (GPa)	$\nu_{12}$	$\nu_{13}$	$\nu_{23}$
AS4/3501-6	132	9.7	9.7	5.9	5.9	3.19	0.28	0.28	0.52
AS4/PEEK	129	10.1	10.1	5.5	5.5	3.43	0.315	0.315	0.47
IM7/977-2	143	9.2	9.2	4.8	4.8	3.067	0.3	0.3	0.5

**Table 5. Parameters for extracting coefficients of failure criteria for laminated composite materials used in the analysis**

Laminated composite materials	$K_{Ic}$ <sup>a</sup> (MPa.m <sup>0.5</sup> )	$-\theta_{0_I}$ <sup>b</sup> (degree)	$-\theta_{0_{II}}$ <sup>b</sup> (degree)	$G_{FPZ_I}$ <sup>a</sup> (kJ/m <sup>2</sup> )	$G_{FPZ_{II}}$ <sup>a</sup> (kJ/m <sup>2</sup> )
AS4/3501-6	1.20	41.81	80.02	0.0561	0.602
AS4/PEEK	3.55	39.70	80.44	0.655	1.09
IM7/977-2	2.04	36.92	80.45	0.324	1.45

<sup>a</sup> Obtained from Refs. [9, 38-42].

<sup>b</sup> Calculated in current study.

**Table 6. Dimensionless coefficients in Eqs. (14), (19) and (31) for different laminated composite materials used in the analysis**

Laminated composite materials	$\rho$	$\rho'$	$\rho''$
AS4/3501-6	1.303	0.306	0.0424
AS4/PEEK	1.382	0.313	0.203
IM7/977-2	1.472	0.305	0.0608

The fracture limit curves extracted by different failure criteria, explained in Section 3 as the mixed mode I/II delamination failure response, are plotted in Figs. 6-8 and compared with the available experimental data of different laminated composite materials.

A comparison of results in these figures clearly indicates that the strain energy density criterion in Eq. (14) is too conservative for all laminated composites, especially when mode II loading is dominant. The first newly proposed failure criterion in Eq. (19), extracted by modifying the crack initiation angle, somewhat improves the results, but still shows a conservative prediction. The main reason is that absorbing energy mechanisms around the delamination tip are ignored in Eq. (19). The simplifying assumption in the extraction of damage factors ( $\rho$  and  $\rho'$ ), which considers the critical strain energy density as an intrinsic material parameter, implies that all energy absorbed by the specimen is consumed for the delamination growth. That is contradictory to the fact that part of the absorbed energy is dissipated through FPZ formation. Hence, as shown in Figs. 6-8, results obtained with the second newly proposed failure criterion in Eq. (31), including the FPZ effects are in good agreement with experimental data. This reveals that this new criterion (unlike

previous ones) due to the consideration of the FPZ effects is more compatible with the nature of delamination phenomena in laminated composite materials.

According to Figs. 5-8, the magnitude of the mode II fracture toughness ( $K_{IIc}$ ) is greater than that the mode I fracture toughness ( $K_{Ic}$ ). This can be attributed to the formation of hackles in the interlaminar zone, which is mainly created in the presence of mode II and perpendicular to the maximum stress direction [23]. This explains why a larger FPZ is created in mode II loading compared to mode I loading [43]. It can be also concluded that adding mode II loading to mode I makes  $K_I$  component more than the mode I fracture toughness ( $K_{Ic}$ ) at low mixed-mode ratios. This can be caused by the activation of mode II toughening mechanisms. The value of  $K_I$  reaches its maximum value at a critical mode mixity. Then, it reduces gradually when mode II becomes more dominant. Due to the common form (elliptical shape) defined for failure criteria, this behavior of the laminated composite materials is not predictable by the proposed criterion, and there is a little difference between the results in the low mode mixity ratios.

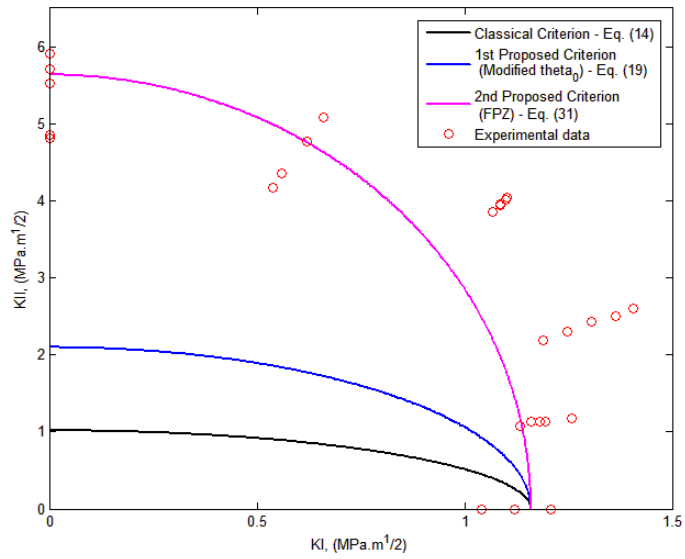
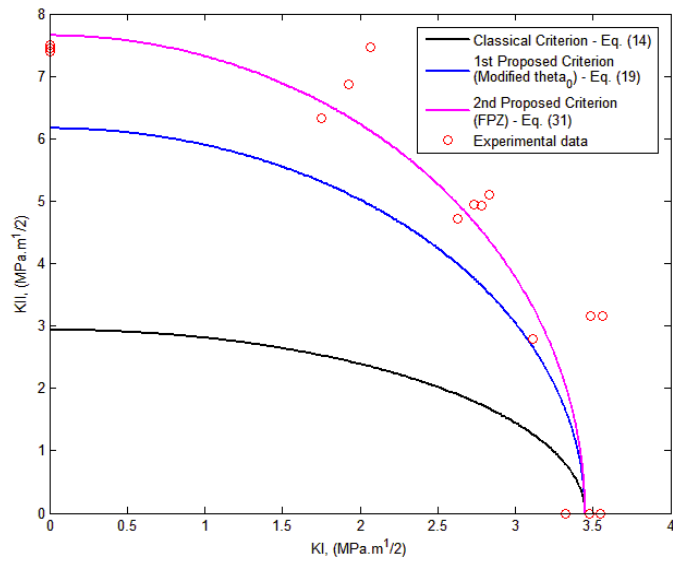
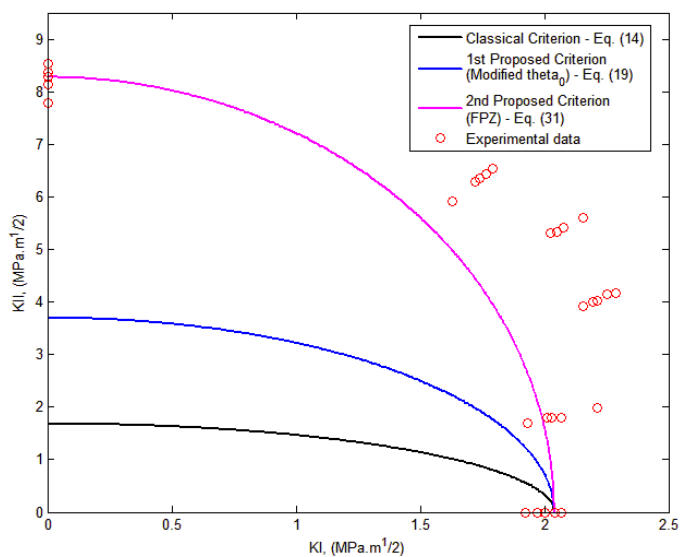


Fig. 6. Fracture limit curves of the failure criteria in comparison with experimental data [9] for AS4/3501-6.



**Fig. 7. Fracture limit curves of the failure criteria in comparison with experimental data [9] for AS4/PEEK.**



**Fig. 8. Fracture limit curves of the failure criteria in comparison with experimental data [9] for IM7/977-2.**

## 5.2. Wood material

Since failure criteria in the present study have been extracted to predict the crack growth in orthotropic materials, the capability of these criteria to investigate the fracture of wood as a natural orthotropic material with principal axes of orthotropy (R, T, L) given by the radial, tangential and longitudinal directions is also evaluated.

To this end, the fracture limit curves obtained by failure criteria in Section 3 (Eqs. (14), (19) and (31)) in comparison with the available experimental data for three wood species, namely Norway spruce, Scots pine and Red spruce with a crack along the wood fibers are shown in Figs. 9-11.

Material properties related to these species are summarized in Table 7. The required parameters and the resulting coefficients of failure criteria are listed in Table 8 and Table 9, respectively.

**Table 7. Material properties of wood species used in the analysis [11, 15]**

Wood species	$E_1 = E_L$ (GPa)	$E_2 = E_R$ (GPa)	$E_3 = E_T$ (GPa)	$G_{12} = G_{RL}$ (GPa)	$G_{13} = G_{TL}$ (GPa)	$G_{23} = G_{RT}$ (GPa)	$\nu_{12} = \nu_{LR}$	$\nu_{13} = \nu_{LT}$	$\nu_{23} = \nu_{TR}$
Norway spruce	11.84	0.81	0.64	0.63	0.61	0.28	0.38	0.56	0.34
Scots pine	16.3	1.10	0.57	1.74	0.67	0.42	0.47	0.45	0.31
Red spruce	12.7	0.98	0.63	0.80	0.74	0.38	0.37	0.42	0.30

**Table 8. Parameters to extract coefficients of failure criteria for wood species used in the analysis**

Wood species	$K_{Ic}$ <sup>a</sup> (MPa.m <sup>0.5</sup> )	$-\theta_{0i}$ <sup>b</sup> (degree)	$-\theta_{0ii}$ <sup>b</sup> (degree)	$G_{FPZ_i}$ <sup>a</sup> (kJ/m <sup>2</sup> )	$G_{FPZ_{ii}}$ <sup>a</sup> (kJ/m <sup>2</sup> )
Norway spruce	0.58	34.25	79.19	0.117	0.277
Scots pine	0.49	44.77	76.70	0.153	0.278
Red spruce	0.42	37.85	78.36	0.125	0.698

<sup>a</sup> Obtained from Refs. [11, 15, 44-47].

<sup>b</sup> Calculated in current study.

**Table 9. Dimensionless coefficients in Eqs. (14), (19) and (31) for wood species used in the analysis**

Wood species	$\rho$	$\rho'$	$\rho''$
Norway spruce	0.829	0.235	0.159
Scots pine	0.389	0.200	0.146
Red spruce	0.747	0.239	0.0498

As can be seen from Figs. 9-11, considering the absorbed energy by micro-cracks formation and growth in FPZ reduces the difference between the criterion and the experimental data. So, the newly proposed criterion (Eq. (31) also has a good correlation with experimental data for wood specimens, whereas two other criteria (Eqs. (14) and (19)) are conservative.

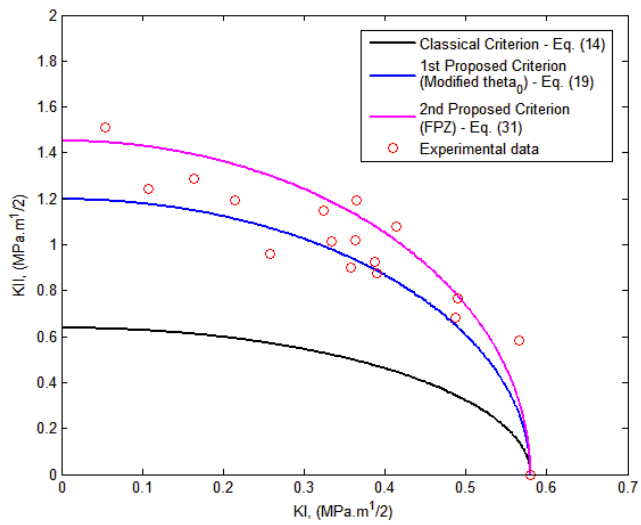


**Fig. 9. Fracture limit curves related to failure criteria in comparison with experimental data [11, 15] for Norway spruce.**

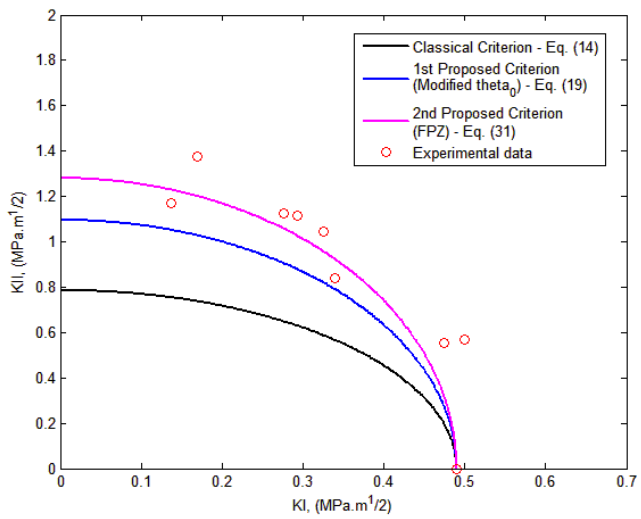


**Fig. 10. Fracture limit curves related to failure criteria in comparison with experimental data [11, 15] for Scots pine.**

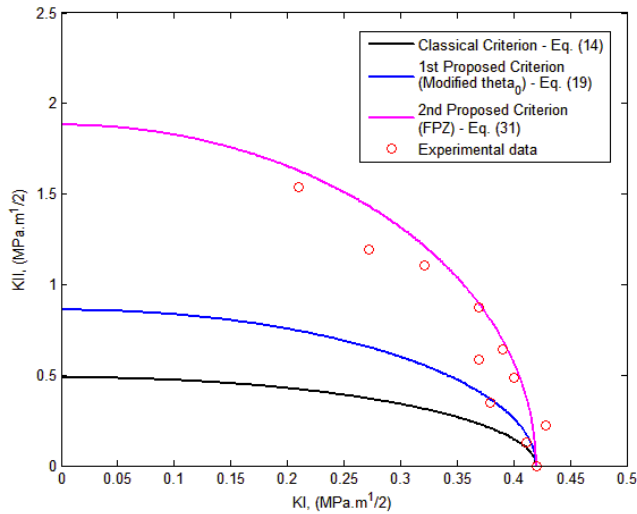


**Fig. 11. Fracture limit curves related to failure criteria in comparison with experimental data [11, 15] for Red spruce.**

## 6. Conclusion

In the present study, a mixed mode I/II failure criterion, based on the strain energy density concept, was presented for prediction of the crack growth in orthotropic materials. First, by eliminating the simplifying assumptions, the minimum strain energy density theory was extended to orthotropic materials. Then, effects of the strain energy density absorbed in the fracture process zone were considered. According to this approach, the newly proposed criterion considers the effects of absorbed energy in the FPZ by defining a suitable damage factor. The mode I fracture toughness, elastic properties of the material and energy absorbed by the fracture process zone are the only

input data required for the criterion. The validity of the present criterion was assessed by comparing the fracture limit curves obtained for various laminated composite materials with the available experimental data. The results are in good agreement with experimental data and show that this criterion is able to estimate the mixed mode I/II delamination failure of laminated composites accurately. The verification of fracture limit curves extracted from the present criterion with the available experimental data of wood species also shows the accuracy of the present criterion.

## References

- [1] Amrutharaja, G.S., Lama, K.Y. and Cotterell, B. "Fracture process zone concept and delamination of composite laminates", *Theor. Appl. Fract. Mech.*, Vol. 24, No.1, pp. 57–64, (1995)
- [2] Shokrieh, M.M., Daneshjoo, Z. and Fakoor, M. "A modified model for simulation of mode I delamination growth in laminated composite materials", *Theor. Appl. Fract. Mech.*, Vol. 82, pp. 107–116, (2016)
- [3] Yao, L., Alderliesten, R., Zhao, M. and Benedictus, R. "Bridging effect on mode I fatigue delamination behavior in composite laminates", *Composites: Part A*, Vol. 63, pp. 103–109, (2014)
- [4] Whitcomb, J.D. "Analysis of Instability-Related Growth of a Through-Width Delamination", NASA TM 86301, September (1984)
- [5] Wu, E.M. and R.C. Reuter, Jr. "Crack extension in fiberglass reinforced plastics", T & AM Report No. 275, University of Illinois, (1965)
- [6] Reeder, J.R. "3D Mixed-Mode Delamination Fracture Criteria– An Experimentalist's Perspective", American Society for Composites 21<sup>st</sup> Annual Technical Conference, Sept (2006)
- [7] Wu, E.M. "Application of fracture mechanics to anisotropic plates", *Journal of Applied Mechanics*, Vol. 34, No.4, pp. 967-974, (1976)
- [8] Mall, S. and Murphy, J.E. "Criterion for mixed mode fracture in wood", *Journal of Engineering Mechanics*, Vol. 109, No.3, pp. 680-690, (1983)

- [9] Reeder, J.R. "A Bilinear Failure Criterion for Mixed-Mode Delamination", in Composite Materials: Testing and Design (Eleventh Volume), ASTM STP 1206, E.T. Camponeschi, Jr., Ed. ASTM Int., W. Conshohocken, PA., pp. 303-322, (1993)
- [10] Benzeggagh, M.L. and Kenane, M. "Measurement of Mixed-Mode Delamination Fracture Toughness of Unidirectional Glass/Epoxy Composites with Mixed-Mode Bending Apparatus", *Comp Sci & Tech*, Vol. 56, No.4, pp. 439-449, (1996)
- [11] Jernkvist, L.O. "Fracture of wood under mixed mode loading: I. Derivation of fracture criteria", *Engng. Fract. Mech.*, Vol. 68, No. 5, pp. 549-63, (2001)
- [12] Griffith, A. A. "The phenomena of rupture and flow in solids", *Phil. Trans. Roy. Soc. London A*, Vol. 221, pp. 163-197, (1921)
- [13] Sih, G. C. "Strain-energy density factor applied to mixed mode crack problems", *Int. J. Fracture*, Vol. 10, No. 3, pp. 305-321, (1974)
- [14] Amaral, L., Alderliesten, R.C. and Benedictus, R. "Towards a physics-based relationship for crack growth under different loading modes", *Eng. Fract. Mech.*, Vol. 195, pp. 222-41, (2018)
- [15] Jernkvist, L.O. "Fracture of wood under mode loading, II: experimental investigation of picea abies", *Eng. Fract. Mech.*, Vol. 68, pp. 565-76, (2001)
- [16] Fakoor, M. and Rafiee, R. "Fracture investigation of wood under mixed mode I/II loading based on the maximum shear stress criterion", *Strength Mater*, Vol. 45, No. 3, pp. 378-85, (2013)
- [17] Romanowicz, M. and Seweryn, A. "Verification of a non-local stress criterion for mixed mode fracture in wood", *Engng. Fract. Mech.*, Vol. 75, No. 10, pp. 3141-60, (2008)
- [18] Anaraki, A.G. and Fakoor, M. "Mixed mode fracture criterion for wood based on a reinforcement microcrack damage model", *Mater Sci Eng, A*, Vol. 527, No. 27, pp. 7184-91, (2010)
- [19] Anaraki, A.G. and Fakoor, M. "A new mixed-mode fracture criterion for orthotropic materials, based on strength properties", *J Strain Anal Eng*, Vol. 46, No. 1, pp. 33-44, (2011)
- [20] Fakoor, M. and Khansari, N.M. "Mixed mode I/II fracture criterion for orthotropic materials based on damage zone properties", *Eng. Fract. Mech.*, Vol. 153, pp. 407-20, (2016)
- [21] Sih, G.C., Paris, P.C. and Irwin, G.R. "On cracks in rectilinearly anisotropic bodies", *Int J Fract Mech*, Vol. 1, No. 3, pp. 189-203, (1965)
- [22] Sih, G.C. *Mechanics of Fracture Initiation and Propagation, Engineering Applications of Fracture Mechanics*, Vol. 11., Springer, Dordrecht, (1991)

- [23] Greenhalgh, E.S., Rogers, C. and Robinson, P. "Fractographic observations on delamination growth and the subsequent migration through the laminate", *Compos Sci Technol*, V. 69, pp. 2345–2351, (2009)
- [24] Budiansky, B. and O'Connell, R.J. "Elastic moduli of a cracked solid", *Int. J. Sol. Struct.*, Vol. 12, pp. 81–97, (1976)
- [25] Feng, X.Q. and Yu, S.W. "Estimate of effective elastic moduli with microcrack interaction effects", *Theoret. Appl. Fract. Mech.*, Vol. 34, No. 3, pp. 225–33, (2000)
- [26] Qiao, P. and Chena, Y. "Cohesive fracture simulation and failure modes of FRP– concrete bonded interfaces", *Theor. Appl. Fract. Mech.*, Vol. 49, No. 2, pp. 213–225, (2008)
- [27] Hillerborg, A. "Analysis of fracture by means of the fictitious crack model, particularly for fiber reinforcement concrete", *Int. J. Cement Compos.*, Vol. 2, pp. 177–184, (1980)
- [28] Suo, Z., Bao, G. and Fan, B. "Delamination R-curve phenomena due to damage", *J. Mech. Phys. Solids*, Vol. 40, No. 1, pp. 1–16, (1992)
- [29] Mai, Y.W. "Cohesive zone and crack-resistance R-curve of cementitious materials and their fiber-reinforced composites", *Eng. Fract. Mech.*, Vol. 69, pp. 219–234, (2002)
- [30] Spearing, S.M. and Evans, A.G. "The role of fiber bridging in the delamination resistance of fiber-reinforced composites", *Acta Metall. Mater*, Vol. 40, pp. 2191–9, (1992)
- [31] Kaute, D.A.W., Shercliff, H.R. and Ashby, M.F. "Delamination, fibre bridging and toughness of ceramic matrix composites", *Acta Metall. Mater.*, Vol. 41, pp. 1959–70, (1993)
- [32] Sørensen, B.F., Gamstedt, E.K., Østergaard, R.C. and Goutianos, S. "Micromechanical model of cross-over fibre bridging – prediction of mixed mode bridging laws", *Mech. Mater.*, Vol. 40, pp. 220–234, (2008)
- [33] Daneshjoo, Z., Shokrieh, M.M. and Fakoor, M. "A micromechanical model for prediction of mixed mode I/II delamination of laminated composites considering fiber bridging effects", *Theor. Appl. Fract. Mech.*, Vol. 94, pp. 46–56, (2018)
- [34] Sun, Z., Hu, Z. and Chen, H. "Effects of aramid-fibre toughening on interfacial fracture toughness of epoxy adhesive joint between carbon-fibre face sheet and aluminum substrate", *Int. J. Adh. Adh.*, Vol. 48, pp. 288–294, (2014)
- [35] Weibull, W. "A statistical theory of the strength of materials", *Proc. Roy. Swed. Inst. Eng. Res.*, Vol. 151, pp. 1–45, (1939)
- [36] Shokrieh, M.M., Zeinedini, A. and Ghoreishi, S.M. "On the mixed mode I/II delamination R-curve of E-glass/epoxy laminated composites", *Composite Structures*, Vol. 171, pp. 19–31, (2017)

- [37] Shokrieh, M.M., Salamat-talab, M. and Heidari-Rarani, M. "Effect of interface fiber angle on the R-curve behavior of E-glass/epoxy DCB specimens", *Theo. Appl. Fract. Mech.*, Vol. 86, pp. 153–160, (2016)
- [38] Hintikka, P., Wallin, M. and Saarela, O. "The effect of moisture on the interlaminar fracture toughness of CFRP laminate", *27<sup>th</sup> International Congress of The Aeronautical Science*, (2010)
- [39] De Moura, M.F.S.F. *Interlaminar Mode II Fracture Characterization*, A volume in Woodhead Publishing Series in Composites Science and Engineering, pp. 310–326, (2008)
- [40] Hojo, M. and Aoki, T. "Characterization of fatigue r-curves based on  $g_{max}$ - constant delamination tests in CF/PEEK laminates", *20<sup>th</sup> International Conference on Composite Materials Copenhagen*, 19-24th July (2015)
- [41] Hojo, M., Matsuda, S., Ochiai, S., Murakami, A. and Akimoto, H. "The role of interleaf/base lamina interphase in toughening mechanism of interleaf-toughened CFRP",
- [42] Cartié1, D., Davies, P., Peleau, M. and Partridge, I.K. "The influence of hydrostatic pressure on the interlaminar fracture toughness of carbon/epoxy composites", *Composites Part B: Engineering*, Vol. 37, No. 4-5, pp. 292-300, (2006)
- [43] Williams, J.G. "On the calculation of energy release rates for cracked laminates", *Int. J. Fract.*, Vol. 36, pp. 101–19, (1988)
- [44] Phan, N.A., Morel, S., Chaplain, M. and Coureau, J-L. "R-curve on fracture criteria for mixed-mode in crack propagation in quasi-brittle material: Application for wood", *Procedia Materials Science*, Vol. 3, pp. 973 – 978, (2014)
- [45] Wilson, E., Shir Mohammadi, M. and Nairn, J.A. "Crack Propagation Fracture Toughness of Several Wood Species", *Advances in Civil Engineering Materials*, Vol. 2, No. 1, pp. 316-327, (2018)
- [46] Morel, S., Mourot, G. and Schmittbuhl, J. "Influence of the specimen geometry on R-curve behavior and roughening of fracture surfaces", *International Journal of Fracture*, Vol. 121, pp. 23–42, (2003)
- [47] Yoshihara, H. "Resistance curve for the mode II fracture toughness of wood obtained by the end-notched flexure test under the constant loading point displacement condition", *J. Wood Sci.*, Vol. 49, pp. 210–215, (2003)